Using x-ray femtoscope and x-ray telescope we verified that dark matter behaves as catalyst or as inhibitor of the nuclear reactions.

Edward Jimenez[1]

[1]Faculty of Chemical Engineering, Central University of Ecuador, Quito-Ecuador. 170521, Gerónimo Leiton S/N y Gatto Sobral. Telf. (5932) 2524766, ehjimenez@uce.edu.ec.

May 17, 2018

Abstract

The X-ray femtoscope predictions: 1.- dark matter has resonances for the chemical elements Cr, Xe and Tm, which corresponds to the forces that gave the name to the WIMPs with ajustment of $\left(R^2 = 0.996\right)$. 2.- Navier Stokes equations and solutions for the atomic nucleus are robust, since they naturally deliver the values of the following constants: neutron radius $r_n = 0.843 fm$, measured for the first time, nuclear viscosity $\left(9.77 * 10^{22} \leq \nu \leq 1.08 * 10^{23}\right) fm^2/s$ and Rydberg constant. 3.- Dark matter produce nuclear catalysis. **The X-ray telescope proofs:** 1.-fluorescent dark matter has resonances in emission and absortion at low X-ray energies $(3.5 KeV)$. 2.- Gravity appears indirectly through the first analytical solution to the millennium problem, associated with the Navier Stokes (NS) equations, which govern the stability of the incompressible nuclear fluid, and which have the range of magnitude of the gravity 10^{-30}. 3.-Dark matter interacts with barionic matter as a catalyst or as an inhibitor, so it is not consumed in the nuclear reaction for Chandra X-Ray Galaxy Clusters at z < 1.4.

1 Introduction

A convergence between the research methods of the atomic nucleus through the x-ray femtoscope is approaching; with the methods of investigation of galaxies, or galaxies cluster through the x-ray telescope *[1], [2]*. Within the similarities we will mention that low energy x-rays are used effectively in the treatment of cancer, in the knowledge of nuclear stability through the solution of the Navier Stokes equations, which is a problem of the millennium and in the characterization of dark matter *[3], [4]*.

At the level of collaborative phenomena, suffice it to mention that one's methodologies have their correspondence in other's methodologies such as, for example, x-ray fluorescence and K edge energies are logically used by the telescope-femtoscope schemes *[5*. The remains of the future will necessarily have to be resolved from the perspective of the integrated cosmos to the quantum perspective.

At the scale of implementation of industrial projects and high scientific impact, it is undeniable the leadership assumed by the x-ray telescopes, which have been put into operation since 1999 in Chandra and XMM Newton and 2016 in Hitomi *[1], [2]*. The galaxies are formed by atoms, the atoms determine the properties of the galaxies and both define the cosmos.

As an added value to the measurement of certain properties of dark matter, in this paper we prove that nuclear stability is a consequence of the equilibrium between forces involved in Navier Stokes equations and nuclear forces and, for this reason, nuclear fluid follows circular trajectories *[5]*. Using NIST published data and GEANT4 Monte Carlo simulations we show that atomic cross section at K-edge resonance is related to nucleon content at each nuclide surface *[6]*. We have considered the atomic nucleus as an incompresible fluid and therefore there is a correlation between physical processes at the surface and inside nucleus. This last was understood in terms of proton and neutron radii measurements with an accuracy given by Rydberg constant, $\left(1.0973731568539(55) * 10^7\right)$. Lastly, we found one solution for the Navier Stokes equations applied to nuclear fluid which can be seen physically as a dynamical generalization of the Yukawa potential and Fermi Dirac distribution.

2 Method.

The atomic nucleus is an incompressible fluid, justified by the formula of the nuclear radius, $R = 1.2A^{\frac{1}{3}}$, where it is evident that the volume of the atomic nucleus changes linearly with $A = Z + N$, giving a density constant. All incompressible fluid and especially the atomic nucleus comply with the Navier Stokes equations. We present a rigorous demonstration on the incomprehensibility of the atomic nucleus, which allows to write explicitly the form of the nuclear force $\mathbf{F}_N = -\frac{g\mu^2}{8\pi}(A-1)P(1-P)\boldsymbol{\nabla}\mathbf{r}$, which facilitates the understanding of nuclear stability.

> To understand the interactions of dark matter with the atomic nucleus, it was necessary to find the solution to one of the problems of the millennium, related to the solution of the Navier Stokes equations.

For our demonstrations, we will use strictly the scheme presented by Fefferman in *http://www.claymath.org/millennium-problems*, where two demonstrations (equations 1,2) are required to accept as valid a solution to the Navier-Stokes 3D equation. *[5]*.

The vector velocity $\mathbf{u}$ defined as $\mathbf{u} = -2\nu\frac{\nabla P}{P}$, with a radius noted as $r = \left(x^2 + y^2 + z^2\right)^{1/2}$ where $P(x, y, z, t)$ is the logistic probability function

$P(x,y,z,t) = \frac{1}{1+e^{kt-\mu r}}$, and the expected value $E(r \mid r \geq 0) < C$ exist. The term P is defined in $\left((x,y,z) \in \mathbb{R}^3, t \geq 0\right)$, where constants $k > 0, \mu > 0$ and $P(x,y,x,t)$ is the general solution of the Navier-Stokes 3D equation, which has to satisfy the conditions (1) and (2), allowing us to analyze the dynamics of an incompressible fluid.

$$\frac{\partial \mathbf{u}}{\partial t} + (\mathbf{u}.\nabla)\,\mathbf{u} = \nu\nabla^2\mathbf{u} - \frac{\nabla p}{\rho_0} \qquad ((x,y,z) \in \mathbb{R}^3, t \geq 0) \qquad (1)$$

Where, $\mathbf{u} \in \mathbb{R}^3$ is a known velocity vector, ρ_0 constant density of fluid, η dynamic viscosity, ν cinematic viscosity, and pressure $p = p_0 P$ in $\left((x,y,z) \in \mathbb{R}^3, t \geq 0\right)$.

Note that velocity and pressure are depending of r and t. We will write the condition of incompressibility.

$$\nabla.\mathbf{u} = 0 \qquad ((x,y,z) \in \mathbb{R}^3, t \geq 0) \qquad (2)$$

2.1 Definitions

Attenuation coefficient.

We will use the known attenuation formula of an incident flux I_0, for which $I = I_0 e^{-\mu r}$. Where, I_0 initial flux and μ attenuation coefficient of energetic photons that enter into interaction and/or resonance with the target atoms, transmitting or capturing the maximum amount of energy.

Growth coefficient.

We will use an equation analogous to concentration equation of Physical Chemistry $C = C_0 e^{kt}$, where $k = \frac{p_0}{2\eta}$, is growth coefficient, p_0 is the initial pressure of our fluid, η the dynamic viscosity and C_0 the initial concentration of energetic fluid atoms.

It is evident that, in equilibrium state we can write $\mu r = kt$, however, the Navier-Stokes equation precisely measures the behavior of the fluids out of equilibrium, so that: $\mu r \neq kt$.

Fortunately, there is a single solution for out-of-equilibrium fluids, using the fixed-point theorem for implicit functions, $\frac{1}{1+e^{kt-\mu r}} = \frac{2}{\mu r}$, the proof is given in Theorem 1. Experimental results can be found in *Figures 1,2*.

Theorem 1 *The velocity of the fluid is given by* $\mathbf{u} = -2\nu\frac{\nabla P}{P}$, *where* $P(x,y,z,t)$ *is the logistic probability function* $P(x,y,x,t) = \frac{1}{1+e^{kt-\mu r}}$, *and* p *pressure such that* $p = p_0 P$, *both defined on* $\left((x,y,z) \in \mathbb{R}^3, t \geq 0\right)$. *The function* P *is the general solution of the Navier Stokes equations, which satisfies conditions (1) and (2).*

Proof. To verify condition (2), $\nabla.\mathbf{u} = 0$, we must calculate the gradients and laplacians of the radius. $\nabla r = \left(\frac{x}{r}, \frac{y}{r}, \frac{z}{r}\right)$, and $\nabla^2 r = \nabla.\nabla r = \frac{\left(y^2+z^2\right)+\left(x^2+z^2\right)+\left(x^2+y^2\right)}{\left(x^2+y^2+z^2\right)^{3/2}} =$

$\frac{2}{r}$.

$$\nabla.u = -2\nu\nabla.\frac{\nabla P}{P} = -2\nu\mu\nabla\left((1-P)\nabla r\right) \tag{3}$$

Replacing the respective values for the terms: $\nabla^2 r$ and $|\nabla r|^2$ in the equation (3).

$$\begin{aligned} \nabla.u &= -2\nu\mu\nabla\left((1-P)\nabla r\right) \\ &= -2\nu\mu\nabla\left((1-P)\nabla r\right) \\ &= -2\nu\mu\left[-\mu(P-P^2)\,|\nabla r|^2 + (1-P)\,\nabla^2 r\right] \end{aligned} \tag{4}$$

Where the gradient modulus of $\nabla P = \mu(P-P^2)\nabla r$, has the form $|\nabla P|^2 = \mu^2(P-P^2)^2\,|\nabla r|^2 = \mu^2(P-P^2)^2$.

$$\nabla.u = -2\nu\mu\,(1-P)\left[-\mu P + \frac{2}{r}\right] = 0 \tag{5}$$

Simplifying for $(1-P) \neq 0$, we obtain the main result of this paper, which represents a fixed point of an implicit function $f(t,r)$ where $f(t,r) = P - \frac{2}{\mu r} = 0$. In Nuclear Physics, $r_0 < r < 1.2A^{1/3}$.

$$P = \frac{1}{1+e^{kt-\mu(x^2+y^2+z^2)^{1/2}}} = \frac{2}{\mu\left(x^2+y^2+z^2\right)^{1/2}} \qquad ((x,y,z)\in\mathbb{R}^3, t\geq 0) \tag{6}$$

Equation (6) has a solution according to the fixed point theorem of an implicit function, and it is a solution to the Navier Stokes stationary equations, which are summarized in: $\nabla^2 P = \frac{2}{\mu}\nabla^2\left(\frac{1}{r}\right) = 0$. Furthermore, it is the typical solution of the Laplace equation for the pressure of the fluid $\nabla^2 p = p_0\nabla^2 P = 0$.

To this point, we need to verify that equation (6) is also a solution of requirement (1), $\frac{\partial\mathbf{u}}{\partial t} + (\mathbf{u}.\nabla)\,\mathbf{u} = \nu\nabla^2\mathbf{u} - \frac{\nabla p}{\rho_0}$. We will do the equivalence $\mathbf{u} = \nabla\theta$ after we replace in equation (1). Taking into account that $\theta = -2\nu\ln(P)$, and that $\nabla\theta$ is irrotational, $\nabla\times\nabla\theta = 0$, we have: $(\mathbf{u}.\nabla)\,\mathbf{u} = (\nabla\theta.\nabla)\,\nabla\theta = \frac{1}{2}\nabla\left(\nabla\theta.\nabla\theta\right) - \nabla\theta\times\left(\nabla\times\nabla\theta\right) = \frac{1}{2}\nabla\left(\nabla\theta.\nabla\theta\right)$, and $\nabla^2\mathbf{u} = \boldsymbol{\nabla}\left(\nabla.\mathbf{u}\right) - \nabla\times\left(\nabla\times\mathbf{u}\right) = \boldsymbol{\nabla}\left(\nabla.\nabla\theta\right) - \nabla\times\left(\nabla\times\nabla\theta\right) = \boldsymbol{\nabla}\left(\nabla^2\theta\right)$. Simplifying terms in order to replace these results in equation (1) we obtain

$$\begin{aligned} (\mathbf{u}.\nabla)\,\mathbf{u} &= \frac{1}{2}\nabla\left(\nabla\theta.\nabla\theta\right) = 2\nu^2\nabla\left(\frac{|\nabla P|^2}{P^2}\right) \\ \nabla^2\mathbf{u} &= \nabla\left(\nabla.\mathbf{u}\right) = \boldsymbol{\nabla}\left(\nabla^2\theta\right) = 0 \\ &= -2\nu\boldsymbol{\nabla}\left(\frac{|\nabla P|^2}{P^2} - \frac{\nabla^2 P}{P}\right) = 0 \end{aligned}$$

The explicit form of velocity is $\mathbf{u} = -2\mu\nu(1-P)\nabla r$. Next , we need the partial derivative $\frac{\partial \mathbf{u}}{\partial t}$

$$\frac{\partial \mathbf{u}}{\partial t} = -2\mu\nu k P(1-P)\nabla r,$$
$$-\frac{\nabla p}{\rho_0} = -\frac{\mu p_0}{\rho_0} P(1-P)\nabla r.$$

After replacing the last four results $(\mathbf{u}.\nabla)\,\mathbf{u}$, $\nabla^2\mathbf{u}, \frac{\partial \mathbf{u}}{\partial t}$ and $-\frac{\nabla p}{\rho_0}$ in equation (1) we obtain (7).

$$-2\mu\nu k P(1-P)\nabla r = 2\nu^2 \nabla\left(\frac{|\nabla P|^2}{P^2}\right) - \frac{\mu p_0}{\rho_0} P(1-P)\nabla r. \tag{7}$$

The equation (7) is equivalent to equation (1). After obtaining the term $\frac{|\nabla P|^2}{P^2}$ from the incompressibility equation $\boldsymbol{\nabla}\left(\nabla^2\theta\right) = -2\nu\boldsymbol{\nabla}\left(-\frac{|\nabla P|^2}{P^2} + \frac{\nabla^2 P}{P}\right) = 0$ and replacing in equation (11).

$$-2\mu\nu k P(1-P)\nabla r = 2\nu^2 \nabla\left(\frac{\nabla^2 P}{P}\right) - \frac{\mu p_0}{\rho_0} P(1-P)\nabla r. \tag{8}$$

Equation (6) simultaneously fulfills requirements (1) expressed by equation (8) and requirement (2) expressed by equation (7), for a constant $k = \frac{p_0}{2\rho_0\nu} = \frac{p_0}{2\eta}$. Moreover, according to equation (6), the probability $P = \frac{2}{\mu r}$ which allows the Laplace equation to be satisfied: $\nabla^2 P = \frac{2}{\mu}\nabla^2\left(\frac{1}{r}\right) = 0$. In other words, the Navier-Stokes 3D equation system is solved. ■

2.2 The nuclear force is related to the Navier Stokes force.

Firstly, we will use the concepts of Classic Mechanics and the formulation of the Yukawa potential, $\Phi(r) = \frac{g}{4\pi r}(A-1)e^{-\mu r}$ to find the nuclear force exerted on each nucleon at interior of the atomic core $\mathbf{F}_N = -\boldsymbol{\nabla}\Phi(r)$. Also, replace the terms of the potential $e^{-\mu r} = \frac{1-P}{P}$ and $\frac{1}{r} = \frac{\mu}{2}P$ by the respective terms already obtained in equation (6).

$$\Phi(r) = \frac{g(A-1)}{4\pi r}e^{-\mu r} = \frac{g\mu(A-1)}{8\pi}(1-P) \tag{9}$$

The general form of the equation (9), is a function of (x, y, z, t).

$$\Phi(r,t) = \frac{g(A-1)}{4\pi r}e^{kt-\mu r} = \frac{g\mu(A-1)}{8\pi}(1-P(r,t)) \tag{10}$$

Secondly, we will obtain the Navier Stokes force equation given by:

$$\frac{d\mathbf{u}}{dt} = \frac{\partial \mathbf{u}}{\partial t} + (\mathbf{u}.\nabla)\,\mathbf{u} = \frac{\partial \mathbf{u}}{\partial t} + 2\nu^2\nabla\left(\frac{|\nabla P|^2}{P^2}\right) = -2\mu\nu k P(1-P)\boldsymbol{\nabla}\mathbf{r} \tag{11}$$

Theorem 2 *The Nuclear Force and Navier Stokes Force are proportional inside the atomic nucleus* $\mathbf{F}_N = C\mathbf{F}_{NS}$.

Proof. Equation (11) rigorously demonstrated by the adequate theorems and propositions, and it represent the acceleration of a particle within the atomic nucleus. According to Classical Mechanics the force of Navier Stokes applied to a particle of mass m, would have the form:

$$\mathbf{F}_{NS} = m\frac{d\mathbf{u}}{dt} = -2m\mu\nu kP(1-P)\boldsymbol{\nabla}\mathbf{r}. \tag{12}$$

The nuclear force on its part would be calculated as follows $\mathbf{F}_N = -\boldsymbol{\nabla}\Phi(r)$.

$$\mathbf{F}_N = -\boldsymbol{\nabla}\Phi(r) = -\frac{g\mu}{8\pi}(A-1)\boldsymbol{\nabla}P. \tag{13}$$

Replacing the term $\nabla P = \mu(P - P^2)\nabla r$, we obtain

$$\mathbf{F}_N = -\boldsymbol{\nabla}\Phi(r) = -\frac{g\mu^2}{8\pi}(A-1)P(1-P)\boldsymbol{\nabla}\mathbf{r}. \tag{14}$$

It is possible to write nuclear force as a function of speed.

$$\mathbf{F}_N = -\boldsymbol{\nabla}\Phi(r) = -\frac{g\mu^2}{8\pi}(A-1)P(1-P)\boldsymbol{\nabla}\mathbf{r}.$$

Finally, we can show that the nuclear force and force of Navier Stokes differ at most in a constant C. Equating (13) and (14), we find the value g as a function of the parameters nuclear viscosity ν, attenuation μ and growth coefficient of the nuclear reaction k, nucleon mass m and $C \neq 1$.

$$g = \frac{16m\pi\nu k}{\mu(A-1)}C \tag{15}$$

■

3 Results.

The main results that are related to the X-ray femtoscope, have to do with the determination of the chemical elements that present resonances in cross section or energy, when interacting with dark matter.

Resonance region. The resonance cross section is produced by interference between the atomic nucleus and the incoming X-rays inside the resonance region, where the boundaries are the surface of the atomic nucleus and K-shell. The equations that allow the calculation of the excess of cross section are the following:

$$\frac{8000\pi\overline{r}\lambda}{(\sigma_2 - \sigma_1)} = R_\infty\left(\frac{\sigma_1}{\sigma_2}\right)^{2.5031}$$

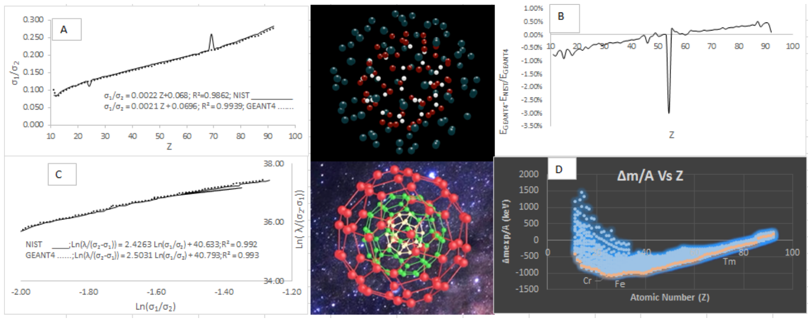

The last equation has a $R^2 = 0.9935$, where $R_\infty = 1.0973731568539(55) * 10^7$ and were obtained and constructed using the elements of the solution of the Navier Stokes equations, *equations (6) and (7)*.

$$\left(\frac{\sigma_1}{\sigma_2}\right) = 0.0021Z + 0.0696$$

This equation was obtained with a $R^2 = 0.9939$, and indicates that the ratio of the cross sections fully explain each element of the periodic table.

$$E = 2 * 10^{-5} Z^2 - 0.0003Z + 0.004$$

This equation obtained for a $R^2 = 0.9996$, complements the system of equations that allow to know the simulation values as a function of Z for $\sigma_1(Z), \sigma_2(Z)$ and $E(Z)$.

By analyzing the graphs $\frac{\sigma_1}{\sigma_2}$ it is clearly concluded that dark matter modifies the cross sections, thus modifying the speed of the nuclear reactions. *Figure 1.*

Figure 1. A.- Calibration of the Femtoscope using the results of GEANT4 and NIST. The linear relationship of the cross sections with the atomic number $11 \leq Z \leq 92$, shows that we can differentiate atomic nuclei, through low energy x-rays (<116 KeV). Resonances in the K edge of the elements Cr and Tm pertmit us to detect dark matter and other irregularities in the atomic nucleus. B.- Resonance of Xe. C.- Calculation of the Rydberg constant. D.- The mass deficit is correlated with the excess cross section for the Cr and the Tm. The question is what implications does this excess mass have? A viable answer has to do with the presence of dark matter near of barionic matter. The images of the atomic nucleus represent the spherical trajectories of nucleon layers, the one with presence of DM and the other without.

Equation (50) is fundamental because it demonstrates that protons and neutrons move in spherical layers, and product of these trajectories creates the nuclear viscosity, *Figure 2*.

The results that have implications with the x-ray telescope, are oriented to determine the speed of the nuclear reactions represented by the speed of the luminosity of the galaxies. The main conclusion is that dark matter behaves as a catalyst or as an inhibitor of nuclear reactions, measured through luminosity, *eq (29) and (30).*

3.1 Cross section and golden ratio $\left(\frac{\sigma_1'}{\sigma_2'}\right)$.

According to NIST and GEANT4, current tabulations of $\frac{\mu}{\rho}$ rely heavily on theoretical values for the total cross section per atom, σ_{tot}, which is related to $\frac{\mu}{\rho}$ by the following equation:

$$\frac{\mu}{\rho} = \frac{\sigma_{tot}}{uA} \tag{16}$$

In (eq. 3), u($= 1.6605402 \times\ 10^{-24}$gr) is the atomic mass unit (1/12 of the mass of an atom of the nuclide 12C)[4].

The attenuation coefficient, photon interaction cross sections and related quantities are functions of the photon energy. The total cross section can be written as the sum over contributions from the principal photon interactions

$$\sigma_{tot} = \sigma_{pe} + \sigma_{coh} + \sigma_{incoh} + \sigma_{trip} + \sigma_{ph.n} \tag{17}$$

Where σ_{pe} is the atomic photo effect cross section, σ_{coh} and σ_{incoh} are the coherent (Rayleigh) and the incoherent (Compton) scattering cross sections, respectively, σ_{pair} and σ_{trip} are the cross sections for electron-positron production in the fields of the nucleus and of the atomic electrons, respectively, and $\sigma_{ph.n}$. is the photonuclear cross section.

We use data of NIST and simulations with GEANT4 for elements Z=11 to Z=92 and photon energies $1.0721 * 10^{-3}$ MeV to $1.16 * 10^{-1}$ MeV, and have been calculated according to:

$$\frac{\mu}{\rho} = \left(\sigma_{pe} + \sigma_{coh} + \sigma_{incoh} + \sigma_{trip} + \sigma_{ph.n}\right)/\mu A \tag{18}$$

$$\sigma_{tot} = \sigma_{coh} + \sigma_{incoh} \tag{19}$$

Resonance region for photons.

A resonance region is created in a natural way at the K-shell between the nucleus and the electrons at S-level. The condition for the photons to enter in the resonance region is given by $r_a \geq r_n + \lambda$. This resonance region gives us a new way to understand the photoelectric effect. There is experimental evidence of the existence of resonance at K-level due to photoelectric effect, represented by the resonance cross section provided by NIST and calculated with GEANT4 for each atom. In the present work we focus on the resonance effects but not on the origin of resonance region.

The resonance cross section is the origin of larger and/or anomaly radiation absorption $\left(I_2 - I_1\right)$.

$$\frac{I_2 - I_1}{\frac{I_2+I_1}{2}} = -\frac{\rho r}{\mu A}\left(\sigma_2 - \sigma_1\right) \tag{20}$$

Lemma 3 *Resonance region. The resonance cross section is produced by interference between the atomic nucleus and the incoming X-rays inside the resonance region, where the boundaries are the surface of the atomic nucleus and K-shell.*

Proof. The cross section of the atomic nucleus is given by:

$$\sigma_{r_n} = 4\pi r_n^2 = 4\pi A^{2/3} r_n^2 \tag{21}$$

The photon cross section at K-shell depends on the wave length and the shape of the atomic nucleus:

$$\sigma_{r_n+\lambda} = 4\pi \left(r_n + \lambda\right)^2 \tag{22}$$

Subtracting the cross sections (22) and (23) we have:

$$\sigma_\lambda = \sigma_{r_n+\lambda} - \sigma_{r_n} = 4\pi \left(2r_n\lambda + \lambda^2\right) = 4\pi \left(2r_p\lambda + 2\left(r_n - r_p\right)\lambda + \lambda^2\right) \tag{23}$$

The resonance is produced by interactions between the X-rays, the K-shell electrons and the atomic nucleus. The cross sections corresponding to the nucleus is weighted by a probability function and should have a simple dependence of an interference term. This last depends on the proton radius r_p or the difference between the nucleus and proton radius $(r_n - r_p)$ according to the following relation ■

$$\left(\frac{\sigma_1}{\sigma_2}\right)^{-b} \left(\sigma_2 - \sigma_1\right) = Max\left(\sigma_2 - \sigma_1\right) = 4\pi\left(2r_p\lambda\right) \tag{24}$$

We note that left hand side of equations (23) and (24) should have a factor larger than one due to resonance. The unique factor that holds this requirement is $\left(\frac{\sigma_1}{\sigma_2}\right)^b$ Where a, b are constants. Figures 3,4.

$$\frac{8\pi\overline{r}\lambda}{\left(\sigma_2 - \sigma_1\right)} = a\left(\frac{\sigma_1}{\sigma_2}\right)^b \tag{25}$$

After performing Geant4 simulations, it is shown that therm a is related to the dimensionless Rydberg constant, $a = \frac{R_\infty}{8000\pi\overline{r}}$ where $R_\infty = 1.0973731568539 * 10^7$. See Figure 3. Similarly, the equivalence of effective cross section is established using equation (53): $\frac{\sigma_1'}{\sigma_2'} = 1 - \left(\frac{\sigma_1}{\sigma_2}\right)^{2.5031}$.

$$\frac{\lambda}{\left(\sigma_2 - \sigma_1\right)} = R_\infty\left(\frac{\sigma_1}{\sigma_2}\right)^{2.5031} \tag{26}$$

Using data of figure 3, we can get the average nucleon radius $\overline{r} = 0.8391$ fm. In the other way, the radius of the neutron can be obtained using equation (26) as follows.

$$
\begin{aligned}
\overline{r} &= \frac{R_\infty}{8000\pi a} \\
r_N &= \frac{A}{N}\overline{r} + \frac{Z}{N}r_p = \phi\overline{r} + \frac{1}{\phi}r_p
\end{aligned}
$$

Using the latest proton radius measurement given $r_p = 0.8335$ fm, for the Max Plank Institute.Therefore, the calculated neutron radius was $r_N = 0.8423$ fm.

Applying the Gaussian Divergence Theorem on the nuclear surface, we can show that the incompressibility property of the nuclear fluid $\overrightarrow{\nabla}.\overrightarrow{u} = 0$, requires to have only spherical trajectories in the equilibrium.

3.2 Spherical trajectory of nucleon layers.

Lemma 4 An action on the nuclear surface produces a reaction in the nuclear volume and vice versa.

Proof. The volume and the nuclear surface are connected through the Gaussian divergence theorem and the Navier Stokes equations. For an incompressible fluid, whose velocity field $\overrightarrow{u}(x, y, z)$ is given, $\overrightarrow{\nabla}.\overrightarrow{u} = 0$ is fulfilled. Logically, the integral of this term remains zero, that is: ■

$$\int\int\int \overrightarrow{\nabla}.\overrightarrow{u}\,dxdydz = 0 \tag{27}$$

Writing the Divergence theorem. $\int\int \overrightarrow{u}.\overrightarrow{n}dS = \int\int\int \overrightarrow{\nabla}.\overrightarrow{u}dxdydz = 0$,, the first term must be equal to zero, that is:

$$\int\int \overrightarrow{u}.\overrightarrow{n}dS = \int\int \|\overrightarrow{u}\|\,\|\overrightarrow{n}\|\cos(\alpha)dS = 0 \rightarrow \alpha = \frac{\pi}{2} \tag{28}$$

The only possible trajectory is circular, because in this case the vector $\overrightarrow{n}$ is perpendicular to the surface of the sphere. In this way the equation of the outer sphere corresponding to the surface is: $x^2 + y^2 + z^2 = 1.2A^{1/3}$. Within the nuclear fluid there are layers of nucleons that move in spherical trajectories.

3.3 Dark matter behave as a catalyst or inhibitor of nuclear reactions.

Proposition 5 *Dark matter acts as a catalyst or inhibitor of nuclear reactions.*

Proof. We must prove that the speed of nuclear reactions increases or decreases through the intervention of dark matter. The relations for stars with different ranges of mass are, to a good approximation, as the following:

$$
\begin{aligned}
\frac{L}{L_{\odot}} &\approx 0.23\left(\frac{M}{M_{\odot}}\right)^{2.3}, \quad \text{when } (M < 0.43M_{\odot}) \qquad (29)\\
\frac{L}{L_{\odot}} &= \left(\frac{M}{M_{\odot}}\right)^{4}, \quad \text{when } (0.43M_{\odot} < M < 0.43M_{\odot})\\
\frac{L}{L_{\odot}} &\approx 1.5\left(\frac{M}{M_{\odot}}\right)^{3.5} \quad \text{when } (2M_{\odot} < M < 20M_{\odot})\\
\frac{L}{L_{\odot}} &\approx 3200\frac{M}{M_{\odot}}, \quad \text{when } (M > 20M_{\odot})
\end{aligned}
$$

Where $L_{\odot}, M_{\odot}$ are luminosity and mass of milky way galaxy. The equations (52), can be simplified as

$$L_M = cq^{\alpha} \qquad (30)$$

with q the fraction (partition) of mass. $q = \frac{M}{M+DM}$.

Processing the data of 81 galaxy clusters, we obtain the information for barionic mass, dark matter and luminosity of the following public sources: Chandra, Hitomi, XMM Newton, https://web.pa.msu.edu/astro/MC2/accept/clusters/3210; html and http://cdsportal.u-strasbg.fr. With one $R^2 = 0.994$, we get the parameters $a = 1.28137(5)$ and $b = -71.4912(0)$.

$$L_{M+DM} = a^{\frac{1}{q}}(1-q)^{b} \qquad (31)$$

Deriving respectively (30) and (31
) with respect to time it is demonstrated:

$$
\begin{aligned}
\frac{q}{\overset{\bullet}{q}}\frac{d\ln(L_{M+DM})}{dt} &\lessgtr \frac{q}{\overset{\bullet}{q}}\frac{d\ln(L_M)}{dt} = cte \qquad (32)\\
-\frac{b}{1-q} - \frac{\ln(L_M^q)}{q} &\lessgtr \alpha = cte
\end{aligned}
$$

With what the proposition is proved. ■

To perform the respective graph of equation (32), we will perform for all the values of q , with $\alpha = 1, 2.3, 3.5, 4.$.

Figure 2. From 78 galaxy clusters processed it is evident that the nuclear reaction speed, represented by the temporal derivative of luminosity, increases or decreases as a function of both the fraction of baryonic matter q and the fraction of dark matter $(1-q)$, (RED). We used public information of Chandra and https://web.pa.msu.edu /astro/MC2/accept/clusters/1652.html. In the image we can visualize perceus, where the fluorescence of dark matter has been studied, which agrees with our results.

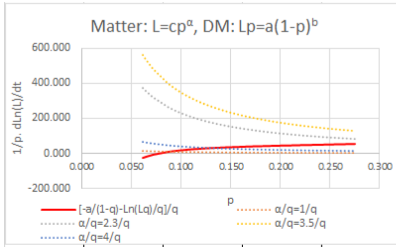

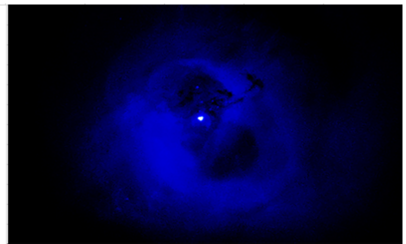

A3921	A3158	A2142	A3112	A 209	PKS0745-191	MACS J0744.8+392	A2244	A 697	A1795
A2034	MKW8	A576	A2597	A3376	ZWCL1215	A496	MACS J0159.8-084	A2256	A1914
MACS J1311.0-0311	A1995	MACS J0011.7-1523	A2029	A3266	A2219	A2163	A3571	A478	A3395
A3558	A644	A1736	A2218	A2052	A 754	A2319	A2124	A3391	A3667
A2147	A 85	A1413	MACS J0429.6-025	A 773	MKW3S	A1664	A 539	A1201	A2390
A 2589	A1835	A2204	A 1068	A2667	A1361	A1651	A2063	A2717	A2199
A2537	A383	A2657	A 401	A119	A521	A907	A1650	MACS J1115.8+0129	A133
A2744	A3562	A2065	A1689	A 262	A1060	A 399	A963		

4 Conclusions

1.-The implementation of the x-ray femtoscope is a direct consequence of the success achieved by the implementation of the x-ray telescope. In addition, it was demonstrated experimentally that the solution of the Navier Stokes equations, continues to be useful to develop models in the x-ray telescope and in the x-ray femtoscope, in the description of dark matter and the nuclear dynamics of galaxies. Fundamentally, it is the missing link between Fluid Dynamics and X-ray spectroscopy.

2.- Some predictions made by the x-ray femtoscope are verified by the x-ray femtoscope and vice versa. At the atomic level, the universe and the stars follow the same laws of Physics-Chemistry. For example, dark matter acts as a catalyst or inhibitor of nuclear reactions, modifying the speed of the reaction, where dark matter is not consumed.

3.-The materials that must be used in the detection of dark matter, are those that have resonance with the atomic nucleus in energy, in cross section or in excess of matter.The big laboratories that investigate dark material, use Xe liquid and are right in this choice, because we have shown that the dark material has resonances in energy K edge, for xenon.

4.-The x-ray telescopes have been implemented since 1999 and have had considerable success in CHANDRA, HITOMI and XMM NEWTON in the characterization and mapping of the universe. However, the x-ray femtoscope complements the research in matter and DM in terms of energy, cross section and resonances in the nuclear surface.

References

[1] Joseph P. Conlon, Francesca Day, Nicholas Jennings et al (2018). Consistency of Hitomi, XMM-Newton, and Chandra 3.5 keV data from Perseus, Phys. Rev. D. (2017).

[2] Yu. V. Babyk, A.Del Popolo and I. B. Vavilova. (2017). Chandra X-Ray Galaxy Clusters at z < 1.4: Constraints on the Inner Slope of the Density Profiles, ISSN 1063-7729, Astronomy Reports, 2014, Vol. 58, No. 9.

[3] Xiao-Jun Yue, Wen-Biao Han. (2018). Dark matter: an efficient catalyst for intermediate -mass -ratio -inspiral events, https://arxiv.org/abs/1802.03739. (2018).

[4] Auerbach. Yeverechyahu 1975, Nuclear viscosity and widths of giant resonances. Annals of Physics. Volume 95, Issue 1, November 1975.

[5] Fefferman (2017). EXISTENCE AND SMOOTHNESS OF THE NAVIER–STOKES EQUATION. http://www.claymath.org /millennium-problems /navier% E2%80%93stokes-equation Accesed 01/05/2017.

[6] Geant 4. (2016). Geant4 User's Guide for Application Developers Version: geant4 10.3. Publication date 9 December 2016.